Connexin 43 plays an important role in the transformation of human cholangiocytes upon stimulation with *Clonochis sinensis* excretory-secretory protein and *N*-nitrosodimethylamine

Short title: Connexin 43 is an important target in human cholangiocarcinoma

Eun-Min Kim[1], Young Mee Bae[2], Min-Ho Choi[2], Sung-Tae Hong[2*]

[1] Department of Environmental Medical Biology and Arthropods of Medical Importance Resource Research Bank, Institute of Tropical Medicine, Yonsei University College of Medicine, Seoul, Republic of Korea

[2] Department of Parasitology and Tropical Medicine and Institute of Endemic Diseases, Seoul National University College of Medicine, Seoul, Republic of Korea

*Corresponding author
E-mail: hst@snu.ac.kr (STH)

.

Abstract

Background

Clonorchis sinensis is a group I bio-carcinogen responsible for cholangiocarcinoma (CHCA) in humans. However, the mechanism by which *C. sinensis* promotes carcinogenesis is unclear.

Methodology

Using the human cholangiocyte line H69, we investigated cell proliferation and gap junction protein expression after stimulation with the hepatotoxin *N*-nitrosodimethylamine (NDMA) and/or excretory-secretory products (ESP) of C. *sinensis*, which induce inflammation. NDMA and ESP treatment increased proliferation by 146% and the proportion of cells in the G2/M phase by 37%. Moreover, the expression of the cell cycle protein E2F1 and the cell proliferation-related proteins Ki-67 and cytokeratin 19 increased in response to combined treatment with NDMA and ESP. The gap-junction proteins connexin (Cx) 43 and Cx26 also increased. In contrast, Cx32 expression decreased in cells treated with NDMA and ESP. Cox-2 was also upregulated. Silencing of Cx43 reduced cell proliferation and significantly suppressed Cx26 and Cox-2 expression.

Conclusions

These results suggest that Cx43 is an important factor in CHCA induced by *C. sinensis* ESP and NDMA and further investigations targeting this pathway may allow prevention of this deadly disease.

Author summary

Clonorchis sinensis, a human fluke, resides in the liver of humans and is commonly found in the common bile duct and gall bladder. This parasite is the main cause of cholangiocarcinoma, also called bile duct cancer, in humans. Of note, the excretory-secretory products (ESP) of *C. sinensis* are known to cause inflammation in the biliary epithelium, which may ultimately result in neoplasms via production of reactive oxygen species and subsequent DNA damage. Together with *N*-nitrosodimethylamine (NDMA), a potent hepatotoxin that can cause fibrosis and tumors in the liver, ESP led to an increase in the growth and proliferation of cholangiocytes. Our results showed that the ESPs of *C. sinensis* induced pro-inflammatory responses by increasing the levels of proinflammatory cytokines and nuclear factor kappa B (NFκB), which in turn, enhanced the production of connexin 43 (Cx43), a gap-junction protein. Therefore, Cx 43 can serve as a potential target for developing a therapeutic strategy for the treatment of cholangiocarcinoma in humans.

Introduction

Clonorchis sinensis is a human liver fluke that induces cholangiocarcinoma (CHCA) in humans [1]. Clonorchiasis has been endemic in Asia for a long time, especially among residents who live along rivers and consume raw

72 freshwater fish [2].

73 The mechanism by which *C. sinensis* induces CHCA is not well
74 understood, but chronic hepatobiliary damage, a precursor to CHCA, in
75 clonorchiasis is a multi-factorial outcome of the mechanical and biochemical
76 irritation of the biliary epithelium by flukes via their suckers, metabolites, and
77 excretory-secretory products (ESP) [3]. Local inflammation and the systemic
78 immune response in the host [4-7] produce reactive oxygen species and
79 reactive nitrogen compounds, which may cause DNA damage, leading to
80 neoplasms [8, 9].

81 *N*-nitrosodimethylamine (NDMA) is a potent hepatotoxin that can cause
82 fibrosis and tumors in the liver of rats via the activation of CYP450 enzymes
83 [10] and hamsters infected with *C. sinensis* are at a greater risk of developing
84 NDMA-induced or inflammation-mediated CHCA than uninfected hamsters
85 [11, 12]. Previously, we reported that exposure to NDMA and the ESP of *C.*
86 *sinensis* increases HEK293T cell proliferation and the proportion of cells in
87 the G2/M phase [3].

88 CHCA is potentially caused by increased levels of proinflammatory
89 cytokines and nuclear factor kappa B (NFκB), which regulate the activities of
90 cyclooxygenase-2 (Cox-2) and inducible nitric oxide synthase, and disturb the
91 homeostasis of oxidants/anti-oxidants and DNA repair enzymes [13]. ESPs of
92 *C. sinensis* induce pro-inflammatory responses *in vitro* by the upregulation of
93 TLR4 and its downstream transduction signals, including MyD88-dependent

94 IκB-α degradation and NFκB activation [14, 15]. NFκB may also influence
95 the production of Cx43, a gap-junction protein, in liver cirrhosis [16, 17].
96 Gap junctions are clusters of transmembrane channels on the cell
97 membrane that permit direct intercellular exchange of ions, secondary
98 messengers, and small signaling molecules influencing cell growth,
99 differentiation, and cancerous changes [17-21]. Among gap junction proteins,
100 Cx43 is involved in almost all steps of the inflammatory response of cells,
101 cytokine production, and inflammatory cell migration [17, 20, 22]. The
102 substantial role of Cx43 in carcinogenesis is highlighted by the fact that high
103 levels of Cx-43 expression increase the invasion of breast tumor cells and
104 promote tumors in melanoma [22].
105 Alterations of Cx expression have been reported in cancer [21, 23]. In
106 hepatocellular carcinoma (HCC), for instance, reduced Cx32 expression is
107 accompanied by increased expression of Cx43, which promotes HCC via cell-
108 to-cell communication [16, 20, 23]. Fujimoto et al. [23] have shown that Cx32
109 has a suppressive effect in metastatic renal cell carcinoma. However, the role
110 of connexins in cancer is still controversial [23], and the influence of gap
111 junctions in CHCA caused by *C. sinensis* has not yet been examined.
112 In this study, to determine the mechanisms underlying the carcinogenic
113 effects of ESP from *C. sinensis,* we investigated changes in cell proliferation,
114 proinflammatory molecules, and connexin production in cholangiocytes (H69
115 cell line) exposed to ESP from *C. sinensis* and the carcinogen NDMA. We

found that the silencing of Cx43 reduced ESP- and NDMA-induced cell proliferation and the expression of Cox-2.

Methods

Preparation of ESP

Animals

The animal experimental protocol was approved and reviewed by the Institutional Animal Care and Use Committee (IACUC) of Seoul National University Health System, Seoul, Korea (approval no. SNU-060511-1) and followed the National Institutes of Health (NIH) guideline for the care and use of laboratory animals (NIH publication no. 85–23, 1985, revised 1996). The facility is accredited by the Ministry of Food and Drug Administration and by the Ministry of Education, Science and Technology (LNL08-402) as an animal experiment facility. Male Sprague–Dawley rats at 6 weeks of age were purchased from Koatech Co. (Seoul, Korea) and housed in an ABL-2 animal facility at Seoul National University College of Medicine. All rats were bred in filter cages under positive pressure according to institutionally approved guidelines.

Recovery of metacercariae of *C. sinensis*

136 *Pseudorasbora parva*, the second intermediate host of C. sinensis,
137 which was naturally infected *with C. sinensis*, was purchased from
138 Sancheong-*gun, Gyeong*sangnam-do, Republic of Korea, an endemic
139 area for clonorchiasis. Metacercariae of *C. sinensis* were collected after
140 the diges*tion of fis*h with pepsin-HCl (0.6%) artificial gastric juice for 1
141 h at 37°C.
142
143 **Infection of experimental animals with *C. sinensis* and collection of**
144 **ESP**
145 Sprague–Dawley rats were individually infected orally with 50
146 metacercariae of *C. sinensis*. Eight weeks post-infection, adult worms
147 were collected from b*ile ducts a*nd washed several times with
148 phosphate-buffered saline (PBS). The freshly isolated worms were then
149 incubated in sterile PBS containing antibiotics for 24 h in an
150 atmosphere of 5% CO_2 at 37°C. After incubation, the medium was
151 centrifuged for 10 min at 800 $_r$pm to remove the worms and debris. The
152 supernatant was then further centrifuged for 10 min at 3000 rpm and
153 filtered with a syringe-driven 0.45-μm filter unit. The amount of protein
154 in each extract was measured using the Bradford assay (Thermo,
155 Rockford, IL, USA). The concentration of endotoxin (LPS) was

156 measured using an LAL QCL-1000 Kit (LONZA, Switzerland), and as
157 a result, the LPS contained in 10 μg/mL of ESP was measured to be
158 less than 0.001 (EU). Therefore, there is no effect of LPS on the results
159 of this paper.
160
161 **Cell culture and experimental design**
162 **Cell culture**
163 SV40-transformed human cholangiocytes (H69) from Dr. Dae-Gon Kim of
164 Chonbuk National University for providing were divided into four treatment
165 conditions and cultured for more than 180 days; the medium was replaced
166 every 72 h. The cells were then treated as follows: control, cultured in plain
167 medium; 100 ng/mL NDMA, cultured in medium containing 100 ng/mL
168 NDMA; ESP, cultured in medium containing 10 μg/mL ESP; and NDMA +
169 ESP, cultured in medium containing 10 μg/mL NDMA and 100 ng/mL ESP.
170 H69 cells were cultured in Dulbecco's modified Eagle's medium (DMEM;
171 Gibco, Carlsbad, CA, USA) and DMEM/F12 supplemented with 10% heat-
172 inactivated fetal bovine serum (FBS; Gibco), 2 mM L-glutamine, 100 μg/mL
173 penicillin, 0.243 mg/mL adenine (Sigma, St. Louis, MO, USA; A68626), 5
174 μg/mL insulin (Sigma; I6634), 10 μg/mL epinephrine (Sigma; E4250), 5
175 μg/mL Triiodonine-transferrin (Sigma; T8158), 30 ng/mL epidermal growth
176 factor (R&D Systems, Minneapolis, MN, USA; 236-EG), 1.1 μM

177 hydrocortisone, and 100 U/mL streptomycin at 37°C in a humidified
178 atmosphere of 5% CO_2.
179
180 **Cell proliferation assay**
181 The PrestoBlue cell viability reagent was utilized to evaluate cell
182 proliferation. For each assay, cells were seeded at a density of 5×10^3
183 cells/well on 96-well plates. After 24 h of incubation, the medium was
184 replaced with 2% FBS-DMEM without phenol red. The cells were then
185 incubated in the presence of PBS (vehicle) or with 100 ng/mL NDMA with or
186 without 10 μg/mL ESP for another 72 h. The PrestoBlue cell viability reagent
187 (1 mg/mL) was dissolved in warm medium, and 1.25 mM phenazine
188 methosulfate (PMS) was prepared in PBS. Following incubation for the
189 indicated periods, 50 μL of the PrestoBlue cell viability reagent was added to
190 each well. The plates were then incubated for 1 h. The conversion of
191 PrestoBlue cell viability reagent was quantified by measuring the absorbance
192 at 570 and 600 nm using a microtiter plate reader.
193
194 **Cell cycle analysis**
195 For the cell cycle analysis, H69 cells were plated in six-well culture
196 plates at 2×10^5 cells/well in 2 mL of DMEM containing 10% FBS. They
197 were then treated with 100 ng/mL NDMA with or without 10 μg/mL ESP for
198 72 h and stained with propidium iodide (PI). The PI-stained cells were

199 analyzed using a FACSCalibur multicolor flow cytometer (Becton-Dickinson,
200 Franklin lakes, NJ, USA), and data were analyzed using CellQuest software
201 (Becton-Dickinson).
202
203 **Western blotting**
204 For western blots, cells were lysed using 1% Nonidet P-40 in a buffer
205 containing 150 mM NaCl, 10 mM NaF, 1 mM PMSF, 200 μM Na_3VO_4, and
206 50 mM HEPES, pH 7.4. Equal amounts of protein were separated by 8% and
207 10% sodium dodecyl sulfate-polyacrylamide gel electrophoresis (SDS-PAGE)
208 and transferred to polyvinylidene fluoride (PVDF) membranes (Immobilon;
209 Millipore, Billerica, MA, USA). The membranes were then probed with
210 antibodies against E2F1, Ki-67, Ck19, Cox-2, connexin 43, connexin 32,
211 connexin 26, and calnexin. The primary antibodies were detected using goat
212 anti-rabbit or rabbit anti-mouse secondary antibodies conjugated with HRP
213 and visualized using an enhanced chemiluminescence kit (ECL; Amersham
214 Pharmacia Biotech, North Massapequa, NY, USA). The western blotting
215 results were obtained by a densitometric analysis using ImageJ (NIH,
216 Bethesda, MD, USA).
217 **Antibodies**
218 Polyclonal or monoclonal antibodies were used to detect the expression
219 of cell-cycle-related proteins, including anti-E2F1 (sc-193; Santa Cruz

220 Biotechnology, Santa Cruz, CA, USA) and anti-Ki-67 (SP6; Abcam,
221 Cambridge, MA, USA). The other antibodies included anti-Cox-2 (c-9897;
222 Cayman Chemicals, Ann Arbor, MI, USA) and anti-cytokeratin-19 (Ab53119;
223 Abcam) as cancer-related makers, and anti-connexin 26 (138100; Invitrogen,
224 Carlsbad, CA, USA), anti-connexin 32 (358900; Invitrogen), and anti-
225 connexin 43 (138300; Invitrogen). An antibody against calnexin (BD 610523)
226 used as a control was purchased from Transduction Laboratories (BD
227 Biosciences, San Jose, CA, USA) and used at a 1:1,000 dilution. Anti-mouse,
228 anti-rabbit, and anti-goat IgG antisera conjugated with horseradish peroxidase
229 (HRP) were purchased from DAKO (Glostrup, Denmark).

230 **Confocal microscopy**

231 Cells were washed with cold PBS three times and fixed with 2%
232 paraformaldehyde in PBS for 30 min. Permeabilization was performed by
233 treating the cells with 0.2% (w/v) Triton X-100 in PBS for 5 min and then
234 blocking with 0.5% BSA in PBS for 1 h. After blocking, the cells were
235 incubated with primary antibodies against connexin 26, 32, and 43 (Invitrogen)
236 diluted in BSA-PBS at 25°C for 2 h and then incubated in secondary
237 antibodies diluted in BSA-PBS at room temperature for 30 min. After
238 washing with 1× PBS, the cells were stained with DAPI and observed under a
239 confocal laser scanning microscope (LSM PASCAL; Carl Zeiss, Jena,
240 Germany).

241

242 **Cx43 silencing with siRNA**

243 Three selected human Cx43-siRNAs (TriFECTa Kit disRNA Duplex,
244 IDT, San Jose, CA, USA), with negative and positive controls, and specific
245 siRNA targeting connexin 43 (NM-00165) (Table 1) were purchased from
246 IDT. The transfection experiments were performed using the TransIT-TKO
247 Kit (Mirus, Madison, WI, USA) following the manufacturer's instructions.
248 Briefly, a 25 nM siRNA solution was mixed with 10 μL of TransIT-TKO and
249 added to the wells of a 6-well plate containing 2×10^5 H69 cells for 72 h.
250 Cells were then treated with NDMA, ESP of *C. sinensis*, or the combination
251 for 72 h. Medium and cells (rinsed 2 times with ice-cold PBS) were harvested
252 3 days later. The efficiency of transfection was assessed by measuring the
253 expression of gap junction proteins (connexin 26, connexin 32, and connexin
254 43) by real-time PCR.

255 Table 1. Connexin43-specific siRNA oligonucleotide sequences

Oligonucleotide name	**Oligonucleotide sequences**
Connexin 43 Duplex	5′-AGCGUUUGCUAUGACCAAUUCUUCC-3′
Sequences	3′-UGUCGCAAACGAUACUGGUUAAGAAGG-5′
Endogenous Gene	5′-GCCAGACUUUGUUGGAUUUGAAATT-3′
Positive Control	3′-AAUUUCAAAUCCAACAAAGUCUGGCUU-5′
Negative Control	5′-CGUUAAUCGCGUAUAAUACGCGUAT-3′

	3′-AUACGCGUAUUAUACGCGAUUAACGAC-5′

Real-time PCR

RNA samples from each cell line were column-purified using the RNeasy Mini Kit (Qiagen, Hilden, Germany). Reverse transcription and real-time PCR (RT-PCR) were performed to determine the mRNA expression levels of *Cx26, Cx32, Cx43*, and *Cox-2*, using *GAPDH* as a control (Applied Biosystems, Santa Clara, CA, USA). The thermal cycling parameters for reverse transcription were modified according to the Applied Biosystems manual. Hexamer incubation at 25°C for 10 min and reverse transcription at 42°C for 30 min was followed by reverse transcriptase inactivation at 95°C for 5 min. cDNA (20 ng) from the previous step was subjected to RT-PCR using specific sets of primers (Table 2 in a total reaction volume of 25 μL (Applied Biosystems). RT-PCR was performed in an optical 96-well plate using an ABI PRISM 7900 HT Sequence Detection System (Applied Biosystems) and TaqMan probe detection chemistry. The running protocol was as follows: initial denaturation at 95°C for 10 min, and 40 cycles of amplification at 95°C for 15 s and 60°C for 1 min. After PCR, a dissociation curve was constructed by increasing the temperature from 65°C to 95°C to evaluate the PCR amplification specificity. The cycle threshold (Ct) value was recorded for each sample.

Table 2. Oligonucleotide primers and detection probe for real-time PCR

Oligonucleotide name	**Oligonucleotide sequences**
Connexin 26	
GJB2 F	CCC CTA AAG CCT CAA AAC AAA G
GJB2 R	GAA ACA AAT GCC GAT ATC CTC TG
GJB2 probe	56-FAM/CCT TAC ACC /ZEN/AAT AAC CCC TAA CAG CCT /3IABkFQ
Connexin 32	
GJB1 F	GCA CAG ACA TGA GAC CAT AGG
GJB1 R	CAA ACC TGT CCA GTT CAT CCT
GJB1 probe	56-FAM/CCT ATC CCT /ZEN/GAG GCC ACC CAG /3IABkFQ
Connexin 43	
GJA1 F	ACT TGG CGT GAC TTC ACT AC
GJA1 R	AGC AGT TGA GTA GGC TTG AAC
GJA1 probe	56-FAM/AGG CAA CAT /ZEN/GGG TGA CTG GAG C/3IABkFQ
Cox-2	
PTGS2 F	ACT TGG CGT GAC TTC ACT AC
PTGS2 R	AGC AGT TGA GTA GGC TTG AAC
PTGS2 probe	/56-FAM/AGG CAA CAT /ZEN/GGG TGA CTG GAG C/3IABkFQ/
GAPDH	

GAPDH F	ACA TCG CTC AGA CAC CAT G
GAPDH R	TGT AGT TGA GGT CAA TGA AGG G
GAPDH probe	5HEX/AAG GTC GGA /ZEN/GTC AAC GGA TTT GGT C/3IABkFQ

Statistical analysis

Statistical significance was analyzed using Student's *t*-tests. Differences were considered statistically significant at a $*P < 0.05$, $**P < 0.01$ and $***P < 0.001$ versus control. Data are presented as the mean ± standard error of the mean (SEM) from at least three independent experiments.

Results

ESP and NDMA synergistically increase H69 cell proliferation

The roles of NDMA and ESP in the proliferation of H69 cells, as determined by cell viability, were investigated. Proliferation was higher in H69 cells treated with NDMA and ESP of *C. sinensis* than in control cells. Compared to control cells, the average increase for cells treated with NDMA was 112%, for cells treated with ESP was 120% ($P < 0.05$), and for cells treated with NDMA + ESP was 146% ($P < 0.001$). NDMA and ESP had synergistic effects on cell proliferation (Fig 1A).

295 **Fig 1: Effects of NDMA and ESP of *C. sinensis* on cell proliferation and**
296 **cell cycle progression in human cholangiocytes (H69 cells). A.** Cells were
297 plated in 96-well plates (5×10^3 cells/well). Cell proliferation for each
298 treatment was determined using the PrestoBlue cell viability assay. **B.** After
299 H69 cells were treated with NDMA and ESP for 72 h, PI staining was
300 performed to determine the percentage of cells in each phase. Data represent
301 the mean ± SE of five independent experiments. $*P < 0.05$, $**P < 0.01$ and
302 $***P < 0.001$ versus control.
303
304 **Cell cycle distribution upon NDMA and/or ESP treatment in H69**
305 **cells**
306 Cell cycle progression was monitored using propidium iodide (PI)
307 staining (Fig 1B). In H69 cells treated with NDMA, ESP, or NDMA + ESP
308 for 72 h, the number of cells in the G0/G1 phase significantly decreased, but
309 cells in the G2/M phase increased significantly compared to cell counts in the
310 control group (Fig 1B). Fewer S-phase cells were identified in the ESP- and
311 NDMA + ESP-treated cells than in control cells. There is no significant
312 increase in G2/M phase in cells treated with NDMA compared to control
313 group (Fig 1B). The proportions of G2/M-phase cells in each condition were
314 as follows: control, 17%; NDMA, 20%; ESP, 26%; NDMA + ESP, 37% ($P =$
315 0.007).
316

Upregulation of inflammation- or transformation-related proteins by NDMA and ESP in H69 cells

Immunoblotting was utilized to detect the regulation of cell-cycle-related proteins in each group using calnexin as a loading control. The expression levels of several cell proliferation- and inflammation-related proteins, including E2F1, Ki-67, Cy-19, and Cox-2 (an essential regulator of the G2/M transition), were upregulated, especially in NDMA + ESP-treated cells (Fig 2).

Fig 2: Expression of inflammation- or transformation-related proteins in H69 cells after treatment with NDMA and ESP, assessed by western blotting. H69 cells were incubated with PBS (vehicle), NDMA, ESP, or both for 72 h. The cells were collected for protein extraction. The blots of each groups were run under same experimental conditions and the images were cropped from different parts of the same gels, DATA represent the mean ± SE of five independent experiments. *$P < 0.05$, **$P < 0.01$ and ***$P < 0.001$ versus control.

Gap junction proteins in H69 cells

The expression levels of Cx26 and Cx43 were high in NDMA + ESP-treated cells, as confirmed by immunoblotting (Fig 3). The intracellular concentrations of Cx26 and Cx43 in each condition were observed under a confocal microscope. Western blotting indicated increases in Cx26 and Cx43

339 expression in cells treated with ESP and NDMA + ESP (Figs 3). The
340 expression of Cx32 (blue) was markedly lower in cells treated with NDMA +
341 ESP than in other cells. Immunofluorescence confocal microscopy indicated
342 that the intracellular concentrations of Cx26 (green) and Cx43 (green)
343 increased in cells treated with NDMA + ESP (Fig 4).
344
345 **Fig 3: Expression of the gap-junction proteins connexin 26, connexin 32,**
346 **and connexin 43 in H69 cells after treatment with NDMA and/or ESP, as**
347 **determined by western blotting.** H69 cells were incubated with either PBS
348 (vehicle) or NDMA and/or ESP for 72 h, and the cells were collected for
349 protein extraction. The blots of each groups were run under same
350 experimental conditions and the images were cropped from different parts of
351 the same gels, DATA represent the mean ± SE of five independent
352 experiments. *$P < 0.05$, **$P < 0.01$ and ***$P < 0.001$ versus control.
353
354 **Fig 4: Concentration of intracellular connexin 26, connexin 32, and**
355 **connexin 43 in human cholangiocytes (H69 cells).** After treatment with
356 NDMA and ESP for 72 h, the concentration of intracellular connexin 26 in
357 H69 cells was measured by laser scanning microscopy (×4,000). Scale bar =
358 25 μm. Data represent the mean ± SE of five independent experiments. *$P <$
359 0.05, **$P < 0.01$ and ***$P < 0.001$ versus control.
360

Reduced cell proliferation upon NDMA and ESP treatment in H69 cells by Cx43 silencing compare to silencing negative control.

Downregulation of Cx43 by Cx43-specific small interfering RNA resulted in all groups were not significant, even though NDMA and ESP stimulated cells. The average increases compared to the control were as follows: NDMA, 104.5%; ESP, 105.1%; and NDMA + ESP, 107.6% (Fig 5A).

Fig 5: Effect of connexin 43 silencing in H69 cells. A. Reduced cell proliferation upon NDMA and ESP treatment in H69 cells by connexin 43 silencing. **B.** Uptake of Cx43 siRNA reduces *Cx43* expression, as confirmed by real-time PCR. *Cx43* expression was remarkably reduced in H69 cells transfected with *Cx43*-specific siRNA. **C.** Ratio of *Cx26/GAPDH* in H69 cells transfected with *Cx43*-specific siRNA. *Cx26* expression was remarkably reduced in H69 cells transfected with *Cx43*-specific siRNA. **D.** The ratio of *Cox-2/GAPDH* in H69 cells transfected with *Cx43*-specific siRNA. *Cox-2* expression was remarkably reduced in H69 cells transfected with *Cx43*-specific siRNA. Data represent the mean ± SE of five independent experiments. *$P < 0.001$ versus control siRNA.

Downregulation of Cx43 by Cx43-specific small interfering RNA reduced the expression of Cx26 and Cox-2 in H69 cells

To evaluate the effect of Cx43 downregulation on the expression of other

383 gap junction proteins and Cox-2, H69 cells were harvested after treatment
384 with NDMA and ESP of *C. sinensis* for 72 h. Transfection with Cx43 siRNA
385 resulted in a reduction in *Cx43* expression of greater than 70% when
386 compared with that of the liposome-only control (Fig 5A). Real-time PCR
387 showed that Cx43 silencing resulted in the downregulation of *Cx26* and *Cox-2*
388 (Figs 5C and 5D, respectively). However, *Cx32* expression was not affected
389 (not shown).
390

391 ## Discussion

392 Our results provided the first evidence for the involvement of gap
393 junction proteins in the pathogenesis of CHCA by *C. sinensis*. NDMA and
394 ESP of *C. sinensis* increased Cx43 expression substantially in H69 human
395 cholangiocytes. In addition, in the presence of ESP and NDMA stimulation,
396 *Cx43* knockdown inhibited *Cox-2* expression in H69 cells. Yan et al. [15]
397 reported that iNOS is highly expressed in Kupffer cells, sinusoidal endothelial
398 cells, and biliary epithelial cells in BALB/c mice after *C. sinensis* infection.
399 Nitric oxide (NO) formation and nitrosation may contribute to the
400 development of *C. sinensis*-associated carcinogenesis [11, 12, 14, 15]. The
401 induction of iNOS under inflammatory conditions suggests that NO is
402 involved in the upregulation of *Cx43* [16, 19]. Therefore, we also expect the
403 involvement of iNOS in the elevation of *Cx43* expression under inflammatory
404 conditions in the present *C sinensis* model. Further studies are warranted to

405 test this hypothesis.

406 Our results indicated that ESP of *C. sinensis* and NDMA had a synergistic
407 effect on the proliferation of human cholangiocytes (Fig 1). In addition to the
408 observed increase in cell proliferation and alteration of the cell cycle, the
409 expression of the gap junction proteins Cx43 and Cx26 increased in H69 cells
410 treated with NDMA and ESP. Most normal cells have functional gap
411 junctional intercellular communication, in contrast to the dysfunctional
412 communication of cancer cells [17-22]. When used in combination with
413 NDMA, ESP of *C. sinensis* induced cell proliferation and increased the
414 expression of E2F1, Ck19, and Ki-67. When H69 cells were co-stimulated
415 with NDMA and ESP, cell proliferation increased. Additionally, as shown in
416 Fig 1B, treatment with NDMA + ESP maximized the proportion of cells in
417 the G2/M phase, implying that NDMA and ESP synergistically stimulate cell
418 cycle progression. We analyzed the expression of a number of cell
419 proliferation-, cell cycle-, and inflammation-related proteins (Fig 2), including
420 E2F1, Ki-67, and Cy19 [24-26]. E2F1 is able to induce cell cycle progression,
421 resulting in cell proliferation [3, 24]. Consistent with these previous findings,
422 we observed that increased expression of E2F1 stimulated cell proliferation.
423 C-Met is involved in early events of carcinogenesis, and Ki-67 is involved in
424 the formation of invasive carcinoma [25-28]. Biliary epithelial cells retain
425 Cy19 expression after neoplastic transformation in almost all cases [26, 28].
426 In our study, Cy19 and Ki-67 were upregulated in response to the stimulation

427 of H69 cell proliferation.

428 Cyclooxygenase 2 (Cox-2), an enzyme involved in the production of
429 prostaglandins, was over-expressed when cells were stimulated by NDMA
430 and ESP. Cox-2 over-expression has been observed in various inflammatory
431 diseases and in bile duct carcinoma cells, mainly in the cytoplasm [29-30].
432 Importantly, bile duct epithelial cells in primary sclerosing cholangitis show
433 very strong Cox-2 expression, comparable to that in carcinoma cells. In
434 contrast, epithelial cells in primary biliary cirrhosis show moderate levels of
435 Cox-2 expression [29, 30]. In this context, the over-expression of Cy19, Ki-67,
436 and Cox-2 may result in the transformation of normal H69 cells to cancer-like
437 cells by stimulation with NDMA and ESP of *C. sinensis*. In the present study,
438 Cx43 and Cx26 expression levels were increased in H69 cells upon
439 stimulation with NDMA and ESP of *C. sinensis*. In contrast, Cx32 was
440 significantly downregulated. Increased expression of hepatic Cx43 was noted
441 in cirrhosis and in a mouse model of acute-on-chronic liver failure in response
442 to LPS, and this effect was related to the severity of inflammation [19]. This
443 increased Cx43 expression was likely an adaptive protective response of the
444 liver to enable better cell-to-cell communication [16, 20, 21]. The expression
445 levels of Cx26 and Cx32, major connexins in the liver, are extremely low in
446 several HCC lines, but Cx43, a minor connexin in the liver, is highly
447 expressed in metastatic cancer [17, 20-22]. Cx43 knockdown using siRNA
448 reduced cell proliferation and significantly suppressed the expression of Cx26

449 and Cox-2 in H69 cells stimulated with NDMA and ESP compare to silencing
450 negative control stimulated with NDMA and ESP. The connexin proteins
451 Cx43 and Cx26 are involved in cell modification upon stimulation by NDMA
452 and ESP of *C. sinensis*.

453 In general, cells contain several known connexins, classified according to
454 their intracellular location (Table 3).

455 Table 3. Full spectrum of connexins expressed in rodent and human livers

Connexins	**Localization**	**References**
Cx26	HP, KC, SC, SEC	Nicholson et al. (1987)
		Zhang and Nicholson (1989)
Cx31.9/Cx30.2	NS	Belluardo et al. (2001)
		Nielsen and Kumar (2003)
Cx32	HP, BEC, SEC	Bode et al. (2002)
		Kumar and Gilula (1986)
		Nicholson et al. (1987)
		Paul (1986)
Cx37	AEC, PEC	Chaytor et al. (2001)
		Saito et al. (2000)
		Shiojiri et al. (2006)
		Willecke et al. (1991)
Cx39	NS	Cicirata et al. (2004)

Cx40	AEC, PEC	Chaytor et al. (2001)
		Shiojiri et al. (2006)
Cx43	AEC, BEC, GC, KC, PEC, SC, SEC	Berthoud et al. (1992)
		Bode et al. (2002)
		Chaytor et al. (2001)
		Shiojiri et al. (2006)

AEC, hepatic artery endothelial cell; BEC, biliary epithelial cell; GC, Glisson's capsule; HP, hepatocyte; KC, Kupffer cell; NS, not specified; PEC, portal vein endothelial cell; SC, stellate cell; SEC, sinusoidal endothelial cell.

Intercellular communication via gap junctions is inhibited by increased Cox-2 expression, as is frequently observed in several forms of human malignancies [29, 30]. Recently, several reports have suggested that the carcinogenic mechanisms of hydrogen peroxide, TPA, and quinones may be involved in the inhibition of GJIC by Cx43 phosphorylation via ERK1/2 activation in rat liver epithelial cells [13, 17]. Furthermore, increased expression of Cx43 is positively correlated with NFκB activation in muscular arteries of patients undergoing coronary artery bypass graft surgery [31]. NFκB plays a central role in general inflammatory and immune responses. The 5′-flanking region of the *Cox-2* promoter contains an NFκB binding site, and NFκB is a critical regulator of Cox-2 expression in many cell lines [13, 31]. Taken together, the present findings suggest that Cx43 expression

induces Cox2 over-expression via NFκB activation. However, until now, the link between NFκB activation, Cx43 expression, and Cox2 over-expression has not been clearly established. In the future, it will be interesting to examine the relationship between the GJIC and NFκB activation, Cox-2 by ESP of *C. sinensis* and NDMA.

In conclusion, our results suggest that Cx43 plays a key role in cell proliferation, potentially leading to CHCA development upon stimulation by ESP of *C. sinensis* and NDMA.

Acknowledgments

We thank Professor Dae-Gon Kim of Chonbuk National University for providing H69 cells. We would like to thank Professor Sung-Jong Hong and Fuhong Dai, Department of Medical Environmental Biology, Chung-Ang University College of Medicine, for providing adult worms of *C. sinensis*.

References

[1] Bouvard V, Barn R, Straif K, Grosse Y, Secretan B, El Ghissassi F, et al. A review of human carcinogens-Part B: biological agents. Lancet Oncol. 2009;10: 321–322.

[2] Kim EM, Kim JL, Choi SY, Kim JW, Kim S, Choi MH, et al. Infection

492 status of freshwater fish with metacercariae of *Clonorchis sinensis* in
493 Korea. Korean J Parasitol. 2008;46: 247-251.
494 [3] Kim EM, Kim JS, Choi MH, Hong ST, Bae YM. Effects of
495 excretory/secretory products from *Clonorchis sinensis* and the carcinogen
496 dimethylnitrosamine on the proliferation and cell cycle modulation of
497 human epithelial HEK293T cells. Korean J Parasitol. 2008;46: 127-132.
498 [4] Kim EM, Bae YM, Choi MH, Hong ST. Cyst formation, increased anti-
499 inflammatory cytokines and expression of chemokines support for
500 *Clonorchis sinensis* infection in FVB mice. Parasitol Int. 2012;61: 124-129.
501 [5] Kim EM, Yu HS, Jin Y, Choi MH, Bae YM, Hong ST. Local immune
502 response to primary infection and re-infection by *Clonorchis sinensis* in
503 FVB mice. Parasitol Int. 2017;66: 436-442.
504 [6] Kim EM, Kwak YS, Yi MH, Kim JY, Sohn WM, Yong TS. *Clonorchis*
505 *sinensis* antigens alter hepatic macrophage polarization in vitro and in vivo.
506 PLoS Negl Trop Dis. 2017;24: 11.
507 [7] Hong ST, Fang Y. *Clonorchis sinensis* and clonorchiasis, an update.
508 Parasitol Int. 2012;61: 17-24.
509 [8] Pinlaor S, Hiraku Y, Ma N, Yongvanit P, Semba R, Oikawa S, et al.
510 Mechanism of NO-mediated oxidative and nitrative DNA damage in
511 hamsters infected with *Opisthorchis viverrini*: a model of inflammation-
512 mediated carcinogenesis. Nitric Oxide. 2004;11: 175-183.
513 [9] Yongvanit P, Pinlaor S, Bartsch H. Oxidative and nitrative DNA damage:

514 key events in opisthorchiasis-induced carcinogenesis. Parasitol
515 Int. 2012;61: 130-135.
516 [10] George J, Murray M, Byth K, Farrell GC. Differential alterations of
517 cytochrome P450 proteins in livers from patients with severe chronic liver
518 disease. Hepatology. 1995;2: 120-128.
519 [11] Lee JH, Rim HJ, Bak UB. Effect of *Clonorchis sinensis* infection and
520 dimethylnitrosamine administration on the induction of
521 cholangiocarcinoma in Syrian golden hamsters. Korean J Parasitol.
522 1993;31: 21-30.
523 [12] Uddin MH, Choi MH, Kim WH, Jang JJ, Hong ST. Involvement of
524 PSMD10, CDK4, and tumor suppressors in development of intrahepatic
525 cholangiocarcinoma of syrian golden hamsters induced by *Clonorchis*
526 *sinensis* and *N*-nitrosodimethylamine. PLoS Negl Trop Dis. 2015;9:
527 e000400.
528 [13] Surh YJ, Lee JY, Choi KJ, Ko SR. Effects of selected ginsenosides on
529 phorbol ester-induced expression of cyclooxygenase-2 and activation of
530 NF-kappaB and ERK1/2 in mouse skin. Ann N Y Acad Sci. 2002;973:
531 396-401.
532 [14] Yan C, Wang YH, Yu Q, Cheng XD, Zhang BB, Li B, et al. *Clonorchis*
533 *sinensis* excretory/secretory products promote the secretion of TNF-alpha
534 in the mouse intrahepatic biliary epithelial cells via Toll-like receptor 4.
535 Parasit Vectors. 2015;8: 559.

536 [15] Yan C, Li B, Fan F, Du Y, Ma R, Cheng XD, et al. The roles of Toll-like
537 receptor 4 in the pathogenesis of pathogen-associated biliary fibrosis
538 caused by *Clonorchis sinensis*. Sci Rep. 2017;7: 3909.
539 [16] Balasubramaniyan V, Dhar DK, Warner AE, Vivien Li WY, Amiri AF,
540 Bright B, et al. Importance of Connexin-43 based gap junction in cirrhosis
541 and acute-on-chronic liver failure. J Hepatol. 2013;58: 1194-1200.
542 [17] Chaytor AT, Martin PE, Edwards DH, Griffith TM. Gap junctional
543 communication underpins EDHF-type relaxations evoked by ACh in the
544 rat hepatic artery. Am. J Physiol Heart Circ Physiol. 2001;280: H2441-
545 H2450.
546 [18] Saito T, Krutovskikh V, Marion MJ, Ishak KG, Bennett WP, Yamaskai H.
547 Human hemangiosarcomas have a common polymorphism but no
548 mutations in the connexin37 gene. Int J Cancer. 2000;86: 67-70.
549 [19] Li K, Yao J, Shi L, Sawada N, Chi Y, Yan Q, et al. Reciprocal regulation
550 between proinflammatory cytokine-induced inducible NO synthase (iNOS)
551 and connexin43 in bladder smooth muscle cells. J Biol Chem. 2011;286:
552 41552-41562.
553 [20] Vinken M, De Kock J, Oliveira AG, Menezes GB, Cogliati B, Dagli ML,
554 et al. Modifications in connexin expression in liver development and
555 cancer. Cell Commun Adhes. 2012;19: 55-62.
556 [21] Bode HP, Wang L, Cassio D, Leite MF, St-Pierre MV, Hirata K, et
557 al. Expression and regulation of gap junctions in rat

558 cholangiocytes. Hepatology. 2002;36: 631-640.

559 [22] Villares GJ, Dobroff AS, Wang H, Zigler M, Melnikova VO, Huang L, et
560 al. Overexpression of protease-activated receptor-1 contributes to
561 melanoma metastasis via regulation of connexin 43. Cancer Res. 2009;15:
562 6730-6737.

563 [23] Fujimoto E, Sato H, Nagashima Y, Negishi E, Shirai S, Fukumoto K, et al.
564 A Src family inhibitor (PP1) potentiates tumor-suppressive effect of
565 connexin 32 gene in renal cancer cells. Life Sci. 2005;76: 2711-2720.

566 [24] Zhu W, Giangrande PH, Nevins JR. E2Fs link the control of G1/S and
567 G2/M transcription. EMBO J. 2004;23: 4615-4626.

568 [25] Sanada Y, Osada S, Tokuyama Y, Tanaka Y, Takahashi T, Yamaguchi K,
569 et al. Critical role of c-Met and Ki-67 in progress of biliary carcinoma. Am
570 Surg. 2010;76: 372-379.

571 [26] Chatzipantelis P, Lazaris AC, Kafiri G, Papadimitriou K, Papathomas TG,
572 Nonni A, et al. Cytokeratin-7, cytokeratin-19, and c-Kit: Immunoreaction
573 during the evolution stages of primary biliary cirrhosis. Hepatol Res.
574 2006;363: 182-187.

575 [27] Tan XP, Zhang Q, Dong WG, Lei XW, Yang ZR. Upregulated expression
576 of Mina53 in cholangiocarcinoma and its clinical significance. Oncol Lett.
577 2012;3: 1037-1041.

578 [28] Aishima S, Nishihara Y, Kuroda Y, Taguchi K, Iguchi T, Taketomi A, et
579 al. Histologic characteristics and prognostic significance in small

580 hepatocellular carcinoma with biliary differentiation: subdivision and
581 comparison with ordinary hepatocellular carcinoma. Am J Surg Pathol.
582 2007;31: 783-791.
583 [29] Hayashi N, Yamamoto H, Hiraoka N, Dono K, Ito Y, Okami J, et al.
584 Differential expression of cyclooxygenase-2 (COX-2) in human bile duct
585 epithelial cells and bile duct neoplasm. Hepatology. 2001;34: 638-650.
586 [30] Lee KW, Chun KS, Lee JS, Kang KS, Surh YJ, Lee HJ. Inhibition of
587 cyclooxygenase-2 expression and restoration of gap junction intercellular
588 communication in H-ras-transformed rat liver epithelial cells by caffeic
589 acid phenethyl ester. Ann N Y Acad Sci. 2004;1030: 501-507.
590 [31] Li JY, Lai YJ, Yeh HI, Chen CL, Sun S, Wu SJ, et al. Atrial gap junctions,
591 NF-kappaB and fibrosis in patients undergoing coronary artery bypass
592 surgery: the relationship with postoperative atrial fibrillation. Cardiology.
593 2009;112: 81-88.
594

A.

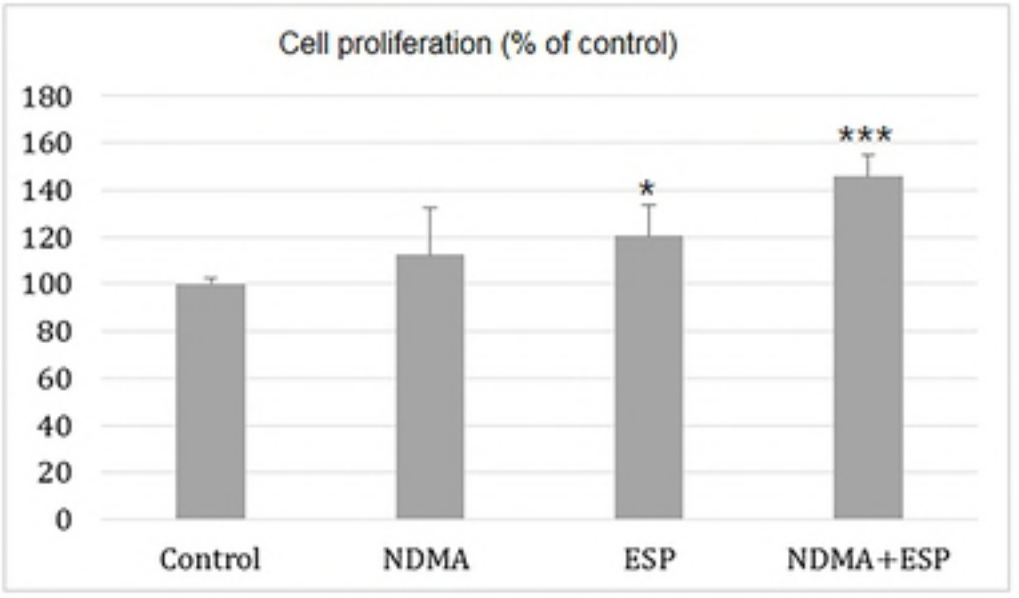
Cell proliferation (% of control)
180
160
140
120
100
80
60
40
20
0
*
***
Control
NDMA
ESP
NDMA+ESP

B.

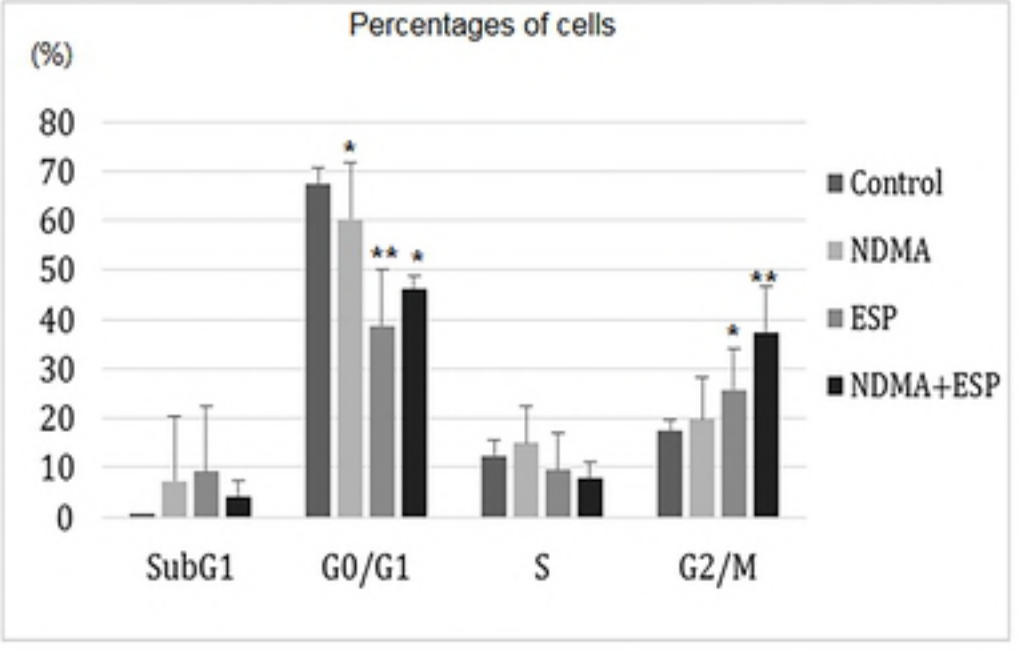
Percentages of cells
(%)
80
70
60
50
40
30
20
10
0
*
**
*
*
**
SubG1
G0/G1
S
G2/M
Control
NDMA
ESP
NDMA+ESP

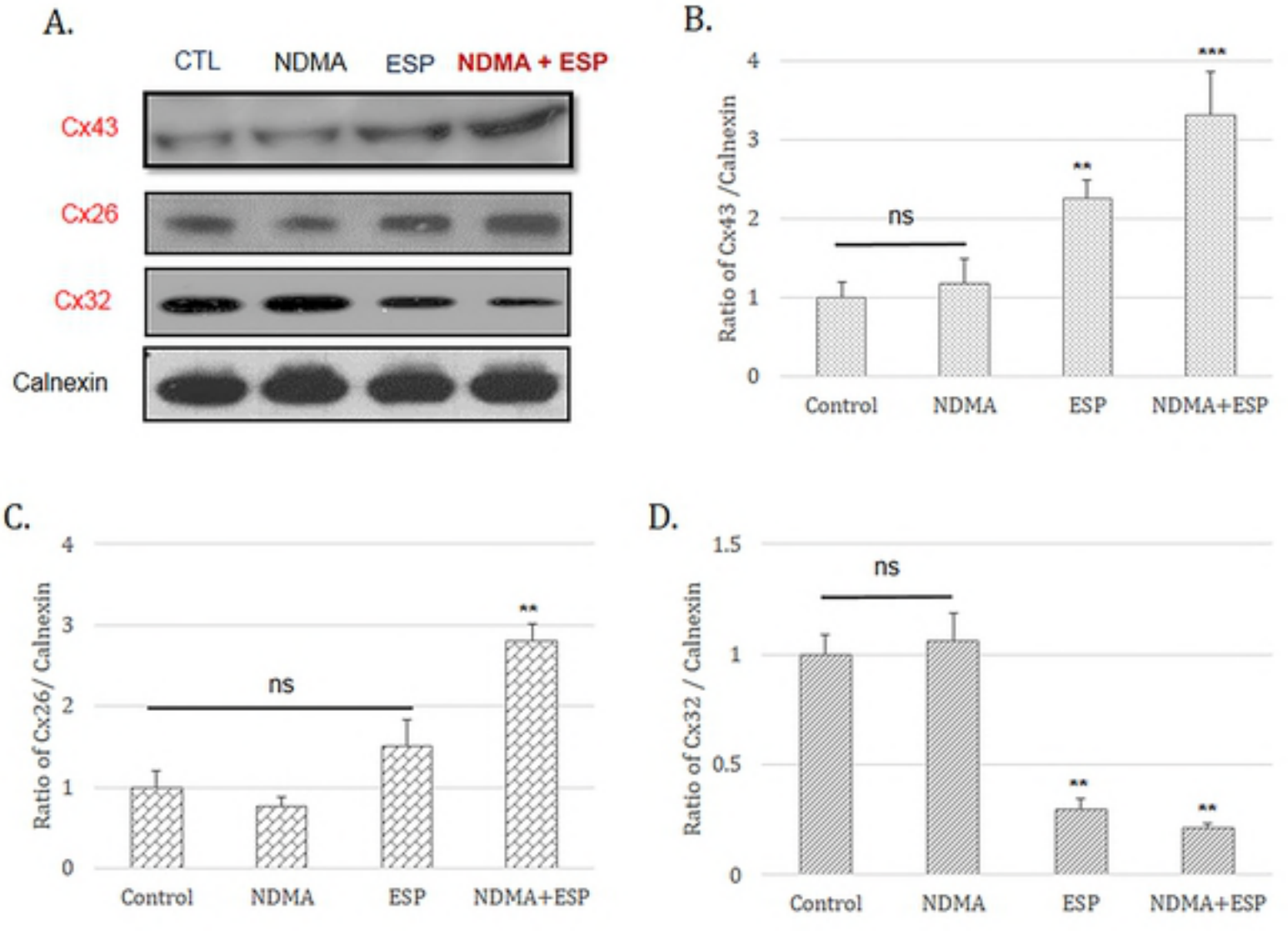
A.
CTL
NDMA
ESP
NDMA + ESP
Cx43
Cx26
Cx32
Calnexin
B.
Ratio of Cx43 /Calnexin
ns
**
***
Control
NDMA
ESP
NDMA+ESP
C.
Ratio of Cx26/ Calnexin
ns
**
Control
NDMA
ESP
NDMA+ESP
D.
Ratio of Cx32 / Calnexin
ns
**
**
Control
NDMA
ESP
NDMA+ESP

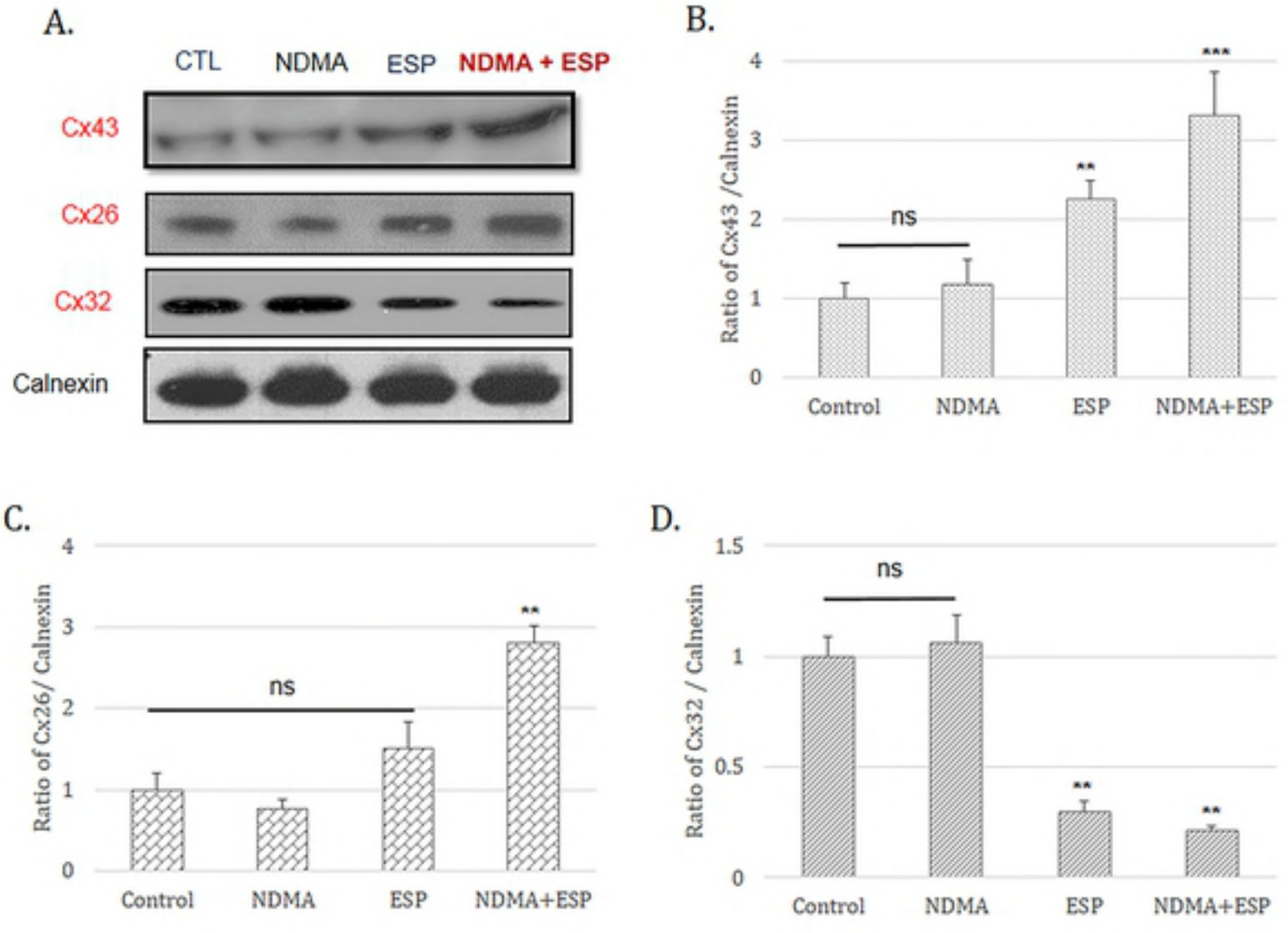
A.
CTL
NDMA
ESP
NDMA + ESP
Cx43
Cx26
Cx32
Calnexin
B.
Ratio of Cx43 /Calnexin
ns
**
***
Control
NDMA
ESP
NDMA+ESP
C.
Ratio of Cx26/ Calnexin
ns
**
Control
NDMA
ESP
NDMA+ESP
D.
Ratio of Cx32 / Calnexin
ns
**
**
Control
NDMA
ESP
NDMA+ESP

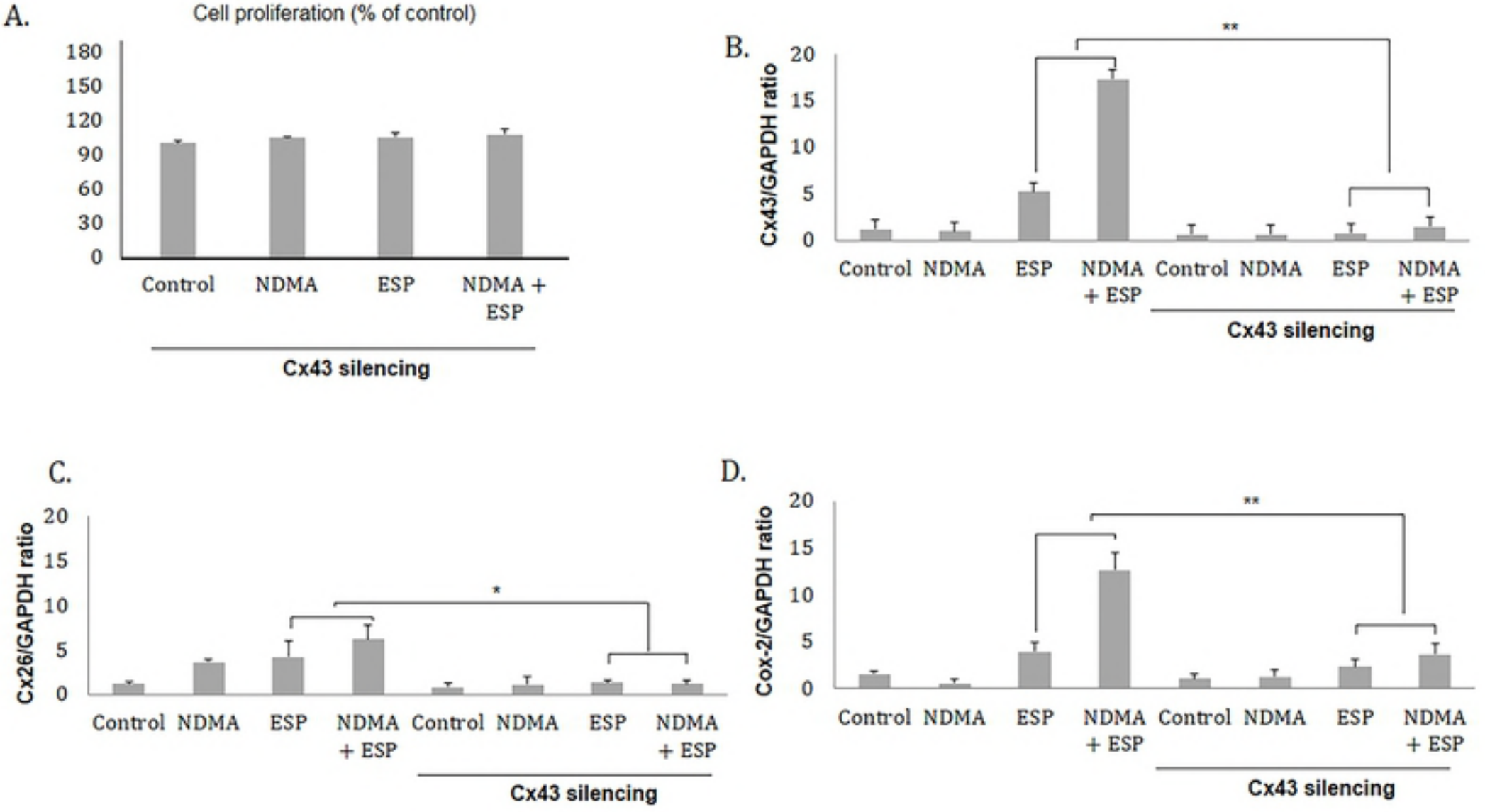
A.
Cell proliferation (% of control)
180
150
120
90
60
30
0
Control
NDMA
ESP
NDMA + ESP
Cx43 silencing
B.
Cx43/GAPDH ratio
20
15
10
5
0
**
Control
NDMA
ESP
NDMA + ESP
Control
NDMA
ESP
NDMA + ESP
Cx43 silencing
C.
Cx26/GAPDH ratio
20
15
10
5
0
*
Control
NDMA
ESP
NDMA + ESP
Control
NDMA
ESP
NDMA + ESP
Cx43 silencing
D.
Cox-2/GAPDH ratio
20
15
10
5
0
**
Control
NDMA
ESP
NDMA + ESP
Control
NDMA
ESP
NDMA + ESP
Cx43 silencing

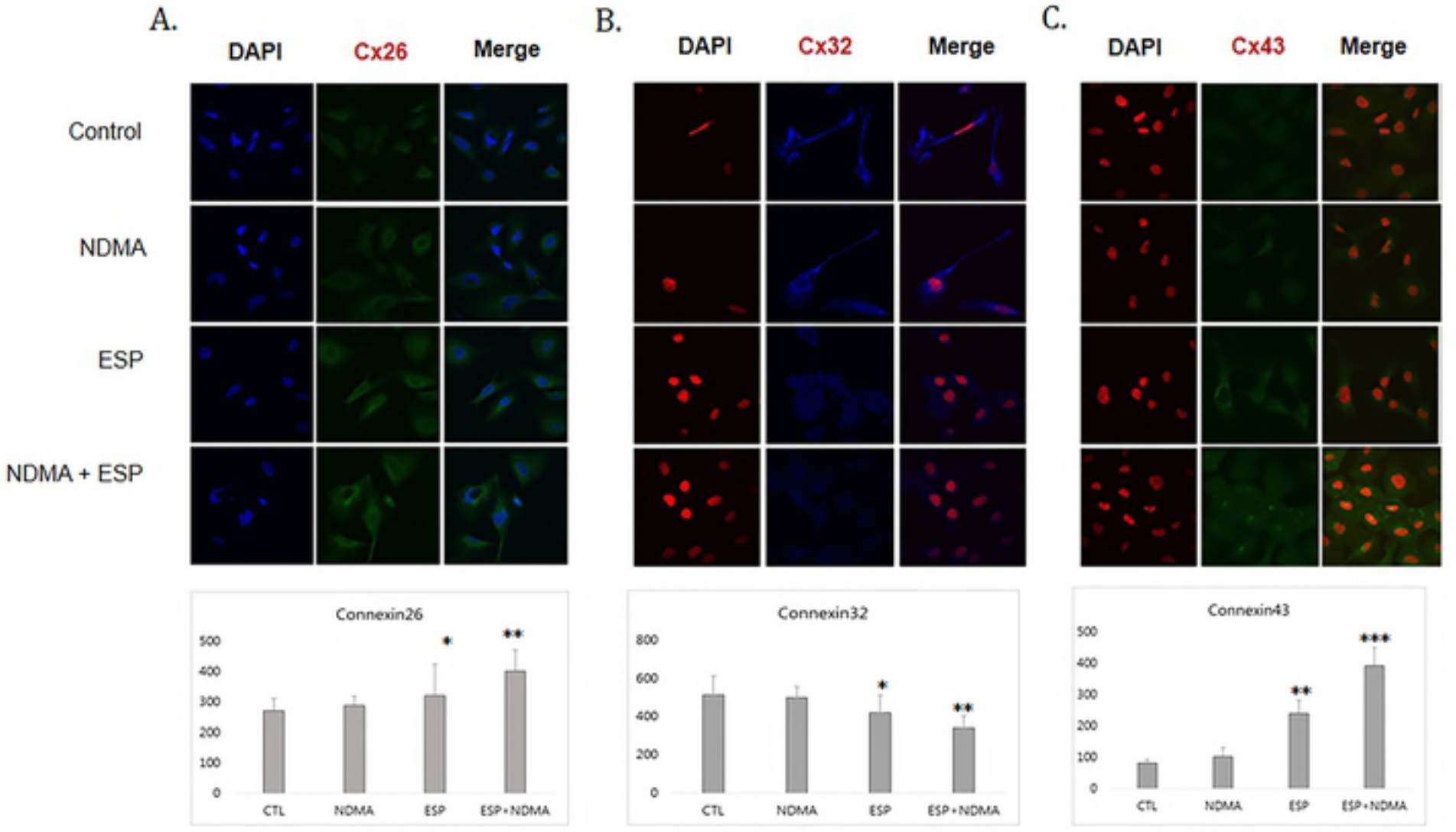
A.
DAPI
Cx26
Merge
Control
NDMA
ESP
NDMA + ESP
Connexin26
500
400
300
200
100
0
*
**
CTL
NDMA
ESP
ESP+NDMA
B.
DAPI
Cx32
Merge
Connexin32
800
600
400
200
0
*
**
CTL
NDMA
ESP
ESP+NDMA
C.
DAPI
Cx43
Merge
Connexin43
500
400
300
200
100
0
**
***
CTL
NDMA
ESP
ESP+NDMA